Biomed Microdevices (2014) 16:897–904
DOI 10.1007/s10544-014-9894-9

Paclitaxel-eluting nanofiber-covered self-expanding nonvascular stent for palliative chemotherapy of gastrointestinal cancer and its related stenosis

Se-Yoon Kim · Mina Kim · Min-kyoung Kim · Haneul Lee · Dong Ki Lee · Don-Haeng Lee · Su-Geun Yang

Published online: 19 August 2014

Abstract Self-expanding non-vascular metal stents (SEMS) is now a choice of treatment for tumor-induced obstructive symptoms of gastrointestinal tract. But in-growing tumor causes re-stenosis. Here, we studied a paclitaxel-eluting nanofiber-covered stent for palliative chemotherapy of gastrointestinal cancer and its related stenosis. *In vivo* and *in vitro* feasibility of nanofiber-covered nonvascular stent was evaluated in this study. Nanofiber-covered stent released paclitaxel (PTX) in controlled manner for 30 days. PTX-NFM significantly inhibited the growth of CT-26 colon cancer in comparison with PTX injection. PTX maintained higher tumor concentrations over 1.0 μg/ml for more than 14 days without systemic exposure. TUNEL and H&E staining proved locally concentrated PTX induced the higher apoptosis than PTX injection. In this way, PTX-eluting nanofiber-covered stent possibly inhibits in-growth of cancer and extends patency of stent. Clinical feasibility of PTX-eluting nanofiber nonvascular stent for cholangiocarcinoma and gastrointestinal cancers will be investigated in further studies.

Keywords Nanofiber · Paclitaxel · Electrospining · Gastrointestinal cancer · Cholangiocarcinoma · Drug-eluting nonvascular stent

1 Introduction

Stents is now the primary choice for treatment of obstruction of humoral ducts, such as blood vessels, bile ducts, the oesophagus, and the colon (Savage et al. 1997; Kang 2010; Kim 2011). Introduction of stent, immediately relieves obstructive symptoms, allows averting an imperative surgery. High cost-effectiveness with low rates of complication is cardinal benefits of stent treatment (Savage et al. 1997; Nicholson 1999). Vascular stents has been exceedingly developed for last decades. Bare-metal stents, replaced balloon angiography, were firstly introduced, and then drug-eluting stents were developed to dissolve restenosis problem of bare metal stent. Now various type of stents (i.e., biodegradable stents, drug-reservoir stents, polymer-free drug coated stents etc.) is under clinical developing (Tsuji et al. 2003; Ramcharitar and Serruys 2008; Khan et al. 2012; Deng et al. 2013) . However restenosis and thrombosis still remain undissolved in vascular stent (Hoffmann et al. 1996; Bennett 2003).

Nonvascular stents were developed for the treatment of benign or malignant strictures of gastrointestinal tract (Thurnher et al. 1996; Kang 2010). The most preferred curative therapy for malignant gastrointestinal obstruction is surgical resection. Unfortunately most of gastrointestinal cancers are diagnosed only when the symptoms are presenting, which means cancer is locally advanced and unresectable. Nonvascular stent to keep gastrointestinal drainage opening is the treatment of choice for unresectable gastrointestinal cancer (Kang 2010; Kim 2011). Gastrointestinal stents are endoscopically introduced inside of lumen at tumoral legion.

Electronic supplementary material The online version of this article (doi:10.1007/s10544-014-9894-9) contains supplementary material, which is available to authorized users.

S.-Y. Kim · M. Kim · D.-H. Lee
Utah-Inha DDS and Advanced Therapeutics Research Center, Incheon 406-840, Republic of Korea
e-mail: sugeun.yang@Inha.ac.kr

M.-k. Kim · H. Lee · D.-H. Lee · S.-G. Yang (✉)
Department of New Drug Development and NCEED, School of Medicine, Inha University, Incheon 400-712, Republic of Korea

D. K. Lee
Department of Internal Medicine, Gangnam Severance Hospital, Yonsei University, Seoul 135-720, Republic of Korea

Plastic stents were firstly introduced for the endoscopic palliation of gastrointestinal cancers followed by self-expandable metallic nonvascular stents (SEMS). Membrane-covered SEMS were most recently introduced (Kim 2011). Metallic nonvascular stents have wire-meshed structure, made from stainless steel or nickel-titanium (nitinol) alloy. Covering-membrane was introduced to overcome ingrowth of tumor through the wire mesh. Chemoresistant materials (i.e., polyurethane, silicone, or polytetrafluoroethylene), which are sustainable against gastric juice or bile acid, have been selected for a covering membrane (Kim 2011).

Restenosis is also problematic issue of nonvascular stents (Kim 2011; Martinez et al. 2011). Tumor infiltrates wire-cage and eventually blocks the passage of body fluids (Davis and Nouneh 2000). The reported patency is around 2.5 to 6.5 months in case of cholangiocarcionoma (Lee et al. 2005). One-third of the patients receive one or more repeated stent replacement. It is here that the development of a cancer-drug eluting stent that inhibits tumor in-growth and extends the patency of the stent is needed for the palliative care of gastrointestinal cancers.

Cancer drug-eluting nonvascular stents have been clinically investigated several times. The first clinical trial of nonvascular DES was performed against 21 patients with unresectable adenomatous esophageal cancer at Guy's Hospital in London (Manifold et al. 1998; Martinez et al. 2011). Stents were coated with ethylene-vinyl acetate (EVA) and 33 % paclitaxel. However, this trial failed to show any clinical effectiveness. More recently, Moon et al. reported the gemcitabine-eluting membrane covered SEMS (Moon et al. 2011). Lee and co-workers inserted paclitaxel-eluting SEMS in porcine bile duct (Lee et al. 2005). Ten percent paclitaxel-loaded film-covered SEMS was prepared by a dipping method. In a similar study, conducted by another group, paclitaxel-eluting SEMS proved to be safe without severe complications in normal canine biliary tracts (Lee et al. 2009). Lei et al. reported 5-fluorouracil-coated film-covered SEMS for esophageal cancer (Lei et al. 2010). In most cases, the stent membrane was fabricated via dip-coating method. But dip-coating cannot assure the uniform drug coating (see supplemental information). In this study, we designed a PTX-eluting electrospun nanofiber membrane (PTX-NFM)-covered nonvascular SEMS. Silicon was selected as primary backing membrane, and PTX-dissolved PU nanofiber was applied as secondary membrane. *In vitro* release of PTX was evaluated in PBS buffer and bile acid solution. And cytotoxic studies were performed on xenograft tumors. Local tissue concentration of PTX on tumor was estimated via LC-MS/MS. Overall results herein motivate the use of PTX-NFM for gastrointestinal interventions associated with cholangiocarcinoma or gastrointestinal cancer, and continued research in preclinical, large animal studies.

2 Materials and methods

2.1 Materials

Paclitaxel (PTX) was obtained from Ningbo Pharmaceutical Technology and Research Co. (Beijing, China). Tetrahydrofuran (THF) and N,N-Dimethylacetamide (DMAc) were purchased from Samchun Chemicals Co. (Seoul, Korea) and Kanto Chemical Co. (Kyoto, Japan). All of the reagents were extra reagent grade and used without any further purification. Polyurethane (PU, Chronoflex® AL 80A, CardioTech International, Inc., MN), non-vascular self-expandable metallic stents (1 cm of diameter and 5 cm length, S biliary stent®, Teawoong medical) and teflon rods were kindly supplied by Taewoong medical (Ilsan, Korea). Paclitalxel injection (PTX-INJ, Genexol-PM®, Samyang Co., Korea) was purchased in the market and used as controls (Kim et al. 2004).

2.2 PTX-eluting nanofiber coating over the stent

We designed a double-layered drug-eluting membrane; silicon backing membrane and drug eluting PU membrane (Fig. 1). A silicone membrane was fabricated by the dipping method (Lee et al. 2005) and pre-activated with Ar-plasma prior to electrospinning (Hsiue et al. 1998). PU (14.5 *w*/*v*%) and PTX (0.5 *w*/*v*%) was dissolved in THF/DMAc (7:3) solution and then electrospun from the syringe at a rate of 0.5 mL/h. The stents were rotated at 300 rpm and increased to 500 rpm over the course of 2–4 h.

2.3 Mechanical properties of PTX-NFM

2.3.1 SEM observation of nanofiber membrane

Surface morphologies of PTX nanofiber membrane (PTX-NFM) were examined by scanning electron microscopy (SEM, Hitachi S-4800, Japan). Stent membranes were sliced into small pieces, mounted, and sputter-coated with gold using an ion coater.

2.3.2 In vitro release study

Whole PTX-NFM was placed inside a 50 mL conical tube with 50 mL of release media (n=6): 10 mM PBS buffer or 10 mM PBS buffer with bile extract. Because we used biliary SEMS for the nanofiber membrane coating, we additionally performed the release study in bile juice media. The bile extract concentration was adjusted to 1,900 ppm, according

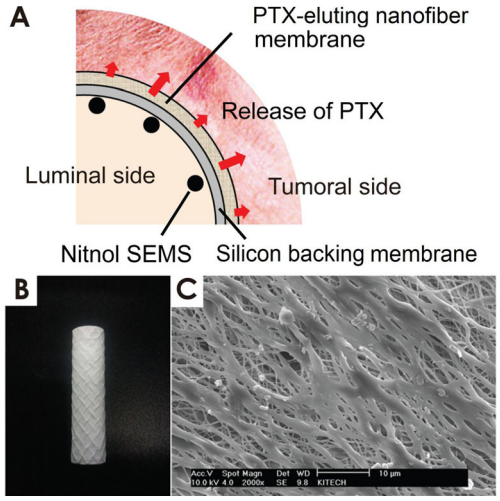

Fig. 1 Paclitaxel (PTX)-eluting nanofiber-covered self-expanding non-vascular stent. (**a**) Pictorial cross section of the PTX-eluting nanofiber-covered SEMS composed of a luminal silicone membrane and an outer PTX-eluting polyurethane (PU) nanofiber layer. The silicone layer directs drug release towards the tumor. (**b**) Photo of the PTX-eluting nanofiber-covered SEMS. (**c**) Scanning electron micrograph of the PU nanofiber membrane

to the reported concentration of human bile juice (Park et al. 2006). The tubes were placed in a shaking incubator at 37 °C and 50 rpm. Media in each tube was collected for analysis and replaced with fresh media at specified times, and the concentration of PTX was determined on a HPLC (Agilent 1200 series, USA).

2.4 Therapeutic and biological properties of PTX-NFM

2.4.1 Cell proliferation inhibition study

CT-26 murine colorectal carcinoma cells were seeded in the acceptor side of Transwell® 6-well, 4.67 cm^2 surface area, 0.4 μm pore size (No. 3450, Corning, NY). After 24 h incubation, blank NFM, the polymeric micelle formulation of PTX (PTX-INJ, Genexol-PM®, Samyang Co., Korea) and PTX-NFM were placed on the donor side of the well. The concentration of PTX was adjusted to 1.2 mg/0.5 ml/well which was the same dose with PTX-NFM. PTX-INJ was applied to the wells for 30 min. and then the cells were washed and incubated with DMEM. The number of proliferating cells was determined on cell suspension at 1, 3 and 5 days of incubation by trypan blue dye exclusion test using an automatic cell counter (ADAM®, Digital Bio, Korea). Cell viability (%) was also calculated by dividing the number of viable cells by the number of total cells.

2.4.2 Flow cytometric measurement of apoptotic cells

Flow cytometry was performed on a BD FACS Calibur (BD Biosciences, USA) flow cytometer. Cell cycle analysis was performed as follows. CT-26 cells ($5x10^5$ cells/well) were inoculated on the acceptor side of the Transwell® plate, incubated for 24 h and treated in the same way as the viability test above (PTX-NFM for 72 h). Cells were collected, resuspended in cold PBS solution and then fixed in ice-cold 70 % ethanol for at least 1 h. The fixing solution was removed, and samples were incubated for 1 h at 37 °C with propidium iodide (10 μg/mL) and ribonuclease A (100 μg/mL) in PBS. Fluorescence intensity of 10,000 cells/sample was determined by flow cytometry, and the data obtained were analyzed using Modfit cell cycle analysis (Immunocytometric System, Becton Dickinson, San Jose, CA, USA).

Cellular apoptosis was determined using annexin V staining kit (Invitrogen). Cells were treated as described above. Cells were then washed twice with cold PBS and then resuspended in 1×Binding Buffer at a concentration of~1×10^6 cells/mL. Then 100 μL of the solution (~1×10^5 cells) was transferred to a 5-ml culture tube. Annexin V and Vital Dye were added and gently mixed with the cells and incubated for 15 min at RT in the dark. 400 μL of 1× Binding Buffer were then added to each tube, and the cells were analyzed by flow cytometry.

2.4.3 In vivo growth inhibition study of xenograft tumor

CT-26 cells (1.0×10^6 cells in 100 μL) were subcutaneously injected on the flank side of female BALB/C mice (Orient Co., Korea). When the tumor grew to an average diameter of~6 mm, the mice were divided into four groups of 6 mice: 1) non-treated, 2) PTX-INJ treated, 3) Blank NFM implanted, and 4) PTX-NFM implanted. Treatment dose was adjusted to 1.2 mg of PTX per mouse. PTX-INJ, Blank NFM and PTX-NFM were sub-tumorally injected or implanted under the tumor. Tumor growth was measured every 2 days using Vernier's calipers (Mytutoyo Co., Japan). Two parameters were measured, the largest perpendicular diameter (a) and the smallest perpendicular diameter (b), and tumor volume was calculated as $V=a\times(b\times b)/2$. All animal care and experimental procedures were conducted in accordance with the guidance for Experimental Animal Research Committee of Inha University.

2.4.4 Tissue concentration of PTX

Concentrations of PTX in tumor, organs and blood from the mice treated with PTX-INJ, Blank NFM and PTX-NFM were measured using LC-MS/MS. Organs and blood were harvested for analysis at 1, 7, 14 and 21 days after treatment. Organ tissues were diluted with distilled water and homogenized. Organ homogenates and aliquots of plasma of (150 μL) were collected in Eppendorf tubes (1.5 mL); 15 μL of docetaxel (1 μg/mL) was added as internal standard. To the tubes, 500 μL of acetonitrile (ACN) was added and centrifuged at

10,000 rpm for 10 min; 500 μL of supernatant was transferred into a fresh tube and completely vacuum-evaporated at 40 °C for 2 h. The residue was reconstituted with 150 μL of mobile phase (ACN, 0.1 % formic acid), filtered and analyzed by LC-MS/MS.

Separation was done using an Agilent 1200 series HPLC system (Agilent Technologies, USA) with a C_{18} column (2.8 μm, 50×2.0 mm) (Persuit XRs ULTRA C18, Varian) at 30 °C. The mobile phase was a linear gradient of water and ACN (with 0.1 % formic acid) at a flow rate of 0.3 mL/min. Mass spectrometry was performed by an API 3200 QTRAP (AB SCIEX, USA) equipped with a turbospray interface operating in positive MRM mode; the transition ions at m/z 854.0 to 286.2 Da for paclitaxel and m/z 830.0 to 549.1 Da for docetaxel Na (IS) were selected for detecting the two compounds. The optimized MRM transition conditions were as follows: ions spray voltage, 5,500 V; source temperature, 400 °C; collision energy, 29 V; curtain gas, 15 psi; nebulizer gas, 50 psi; auxiliary gas, 35 psi.

2.4.5 Histological observation of tumors

Tumors were harvested at 1 and 14 days post membrane insertion and stained with hematoxylin-eosin (H&E) and by terminal dUTP nick end labeling (TUNEL). Staining was performed by the routine protocol after paraffin embedding. Samples were examined on a light microscope (Leica MD 2500, Germany). TUNEL assay was performed according to the manufacturer's protocol (TUNEL apoptosis detection kit, Millipore, Germany). The prepared tissue samples were mounted on slide glasses and observed on a fluorescence microscope (Axio Observer, Carl Zeiss Co., Germany)

3 Result and discussion

3.1 Physical properties of PTX-eluting nanofibers

As mentioned before, the drug eluting membranes were constructed with two layers (Fig. 1a): a primary silicone layer coated by a paclitaxel-eluting nanofiber. The silicone membrane functionally designed (1) as a basal membrane to enhance the mechanical strength of the stent membrane and (2) as a physical barrier that directs the release of PTX towards malignant tissue. As seen in Fig. 1b and c, the PU nanofibers fabricated by electrospinning formed a homogenous, fine woven mesh with around 1 μm of diameter (Park et al. 2012).

Release of PTX from PTX-NFM was monitored for 30 days (Fig. 2). Daily delivery dose of PTX should be controlled enough to inhibit tumor in-growth. Membrane thickness of gastrointestinal stents should be precisely controlled for easy deployment from endoscopic delivery catheter. PTX-NFM has around 50 to 70 μm of thickness. Controlled release of PTX from such thin membrane under the corrosive gastrointestinal

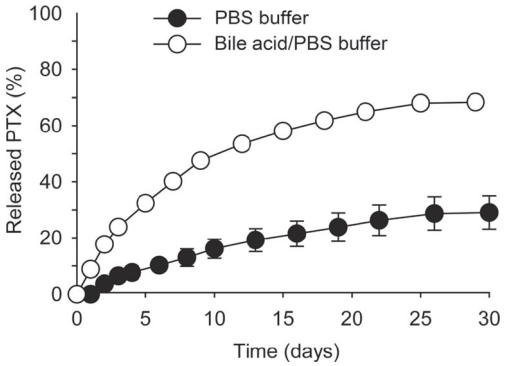

Fig. 2 The sustained release of PTX from PU nanofiber membrane (n= 6). Closed circles; PBS buffer, open circles; bile acid-containing PBS buffer which mimics the circumstance of bile duct stent for palliative chemotherapy of cholangiocarcinoma (Park et al. 2006)

environments (i.e., bile acid, digestive enzyme, gastric acid and food debris) is hardly attainable. Fortunately, PTX-NFM showed steady release of PTX without an initial burst. PTX concentrations were 6.48±0.50 μg/cm^2/day for 10 days and 1.28±0.01 μg/cm^2/day for the following 20 days in PBS buffer containing 1,200 ppm of bile extract. The releasing half-life ($T_{2/1}$) of PTX-NFM was 9.09±0.36 h and 5.47±0.04 h in PBS and in bile juice media, respectively.

3.2 *In vitro* antitumor efficacy of PTX-eluting nanofiber

Antitumor efficacy of PTX-NFM was evaluated by an *in vitro* tumor cell growth inhibition assay (Fig. 3 and Fig. S4). CT-26 cells are a murine colorectal cancer cell line, and serve as a model for these colorectal stents. They were treated with polymeric micelle formulations of PTX (PTX-INJ), Blank NFM, and PTX-NFM. A PTX-INJ concentration of 1.2 mg per well was applied to the cells for 30 min, then the cells were washed with PBS and incubated with DMEM.

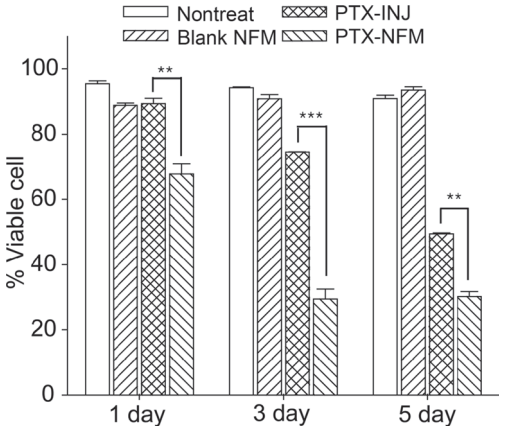

Fig. 3 Cell viabilities (%) of CT-26 murine colorectal cancer cells treated with blank nanofiber membrane (NFM), PTX-inj. and PTX-NFM. Cell viability was calculated by dividing the viable cell number by the total cell number, multiplied by 100 %. The numbers of viable cells and total cells were measured by trypan blue exclusion test. *P*-values were calculated with student *t*-test: **p<0.01, ***p<0.001

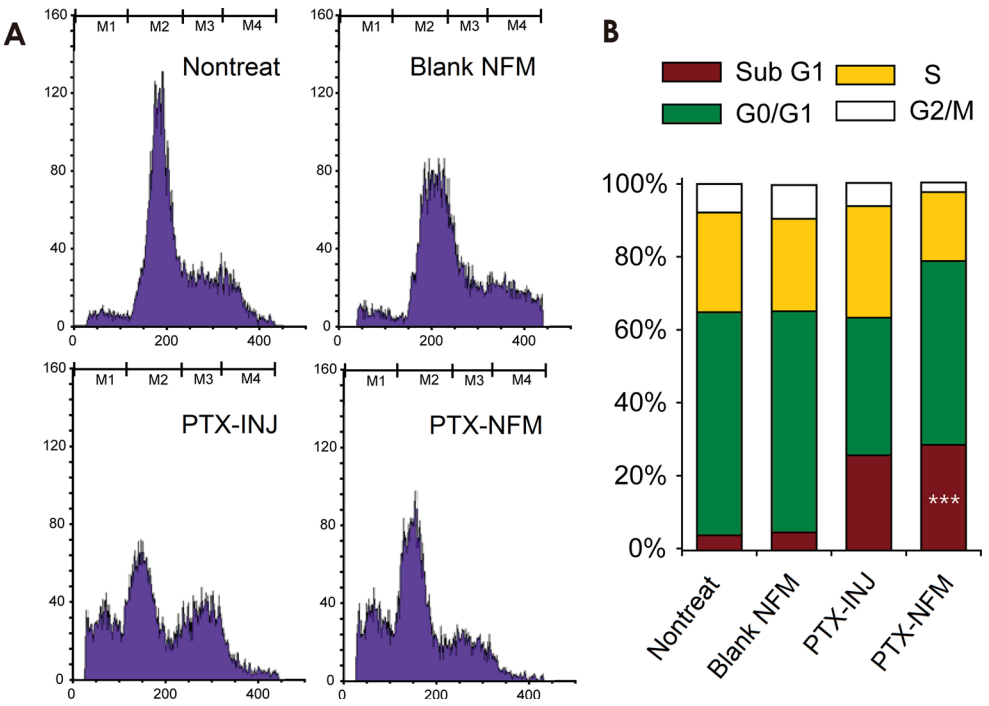

Fig. 4 Flow cytometry of CT-26 cells treated with blank NFM, PTX-INJ. and PTX-NFM: (**a**) ploidy analysis and (**b**) cell cycle populations. Treatment with PTX-INJ and PTX-NFM showed increased populations of cells in the Sub G1 phase, indicative of increased cell apoptosis. ***$p<0.001$ between NFM and PTX-NFM

Figure 3 shows that non-treated and NFM-treated cells maintained over 90 % viability during the experiment. The PTX-INJ treated cells showed decreased cell viabilities of 74.5 and 49.5 % at days 3 and 5, respectively. The PTX-NFM treated cells showed decreased cell viability from day 1 at 67.8 %, with 29.4 and 30.2 % on days 3 and 5, respectively. The PTX-NFM showed greater antitumor activity on day 3 with a 45.1 % difference with respect to PTX-INJ. On day 5, a 19.3 % difference between PTX-NFM and PTX-INJ is observed. This data demonstrates the effectiveness of continuous drug delivery (PTX-NFM) directed to a local environment versus the burst drug delivery (PTX-INJ) of bolus injections, and underscores the need for controlled drug release kinetics.

Flow cytometry was used to examine the apoptotic status of CT-26 cells under each treatment. PTX works as a microtubule stabilizer, which in turn inhibits mitotic division and

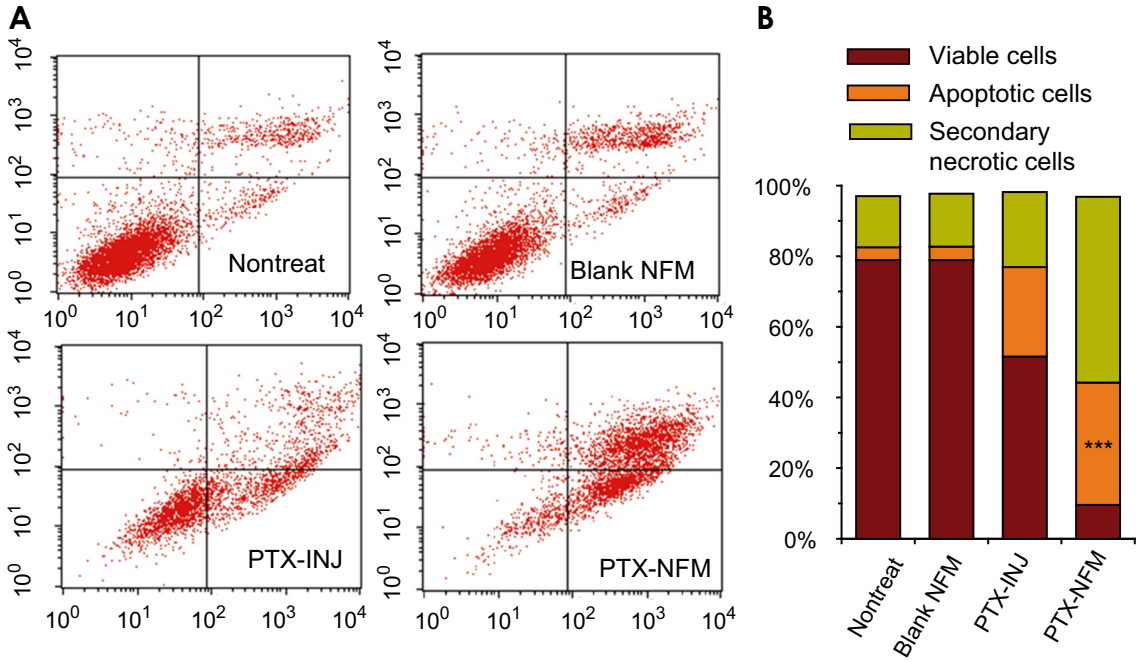

Fig. 5 Apoptotic activity of blank NFM, PTX-INJ and PTX-NFM treated CT-26 murine colon cancer cells: (**a**) scatter plot and (**b**) histogram analysis. ***$p<0.001$ between NFM and PTX-NFM

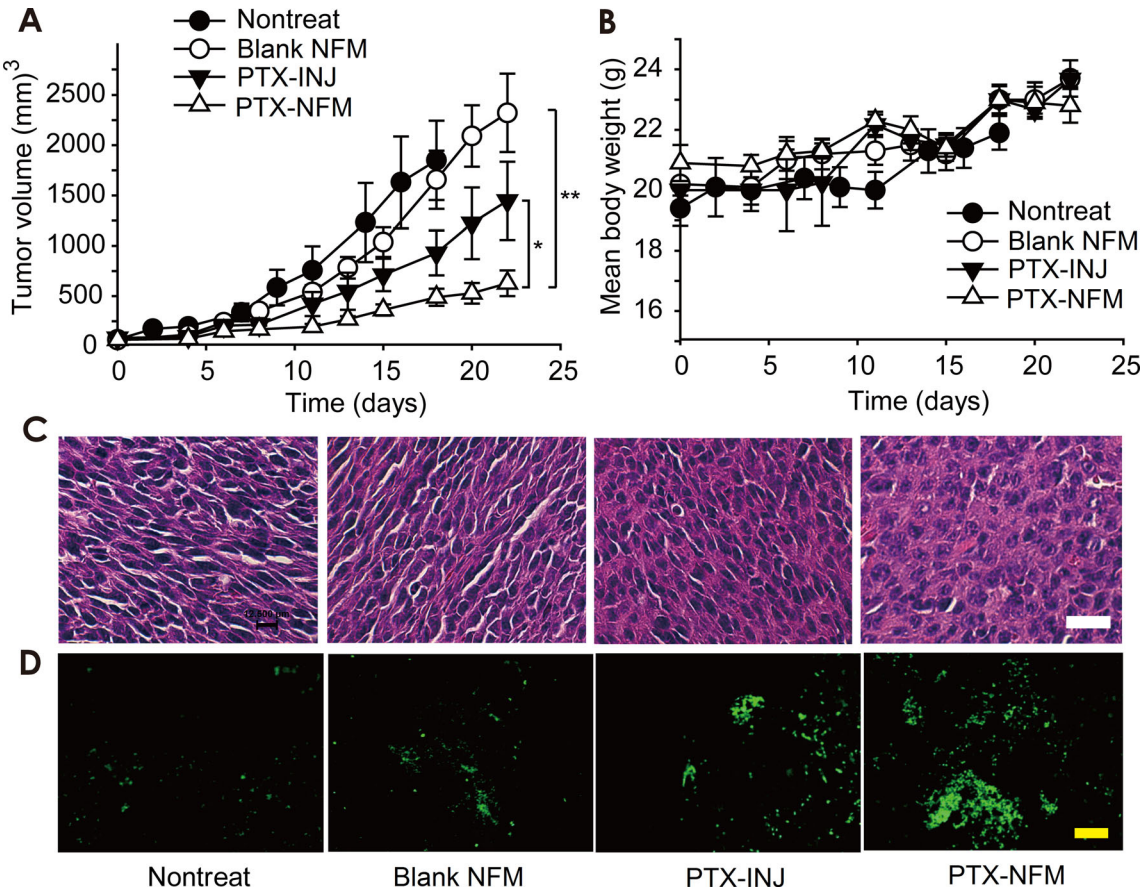

Fig. 6 *In vivo* inhibition of tumor growth (**a**), body weight changes (**b**) and tumor histology (**c**, **d**). PTX-NFM significantly inhibited the xenografted CT-26 tumor growth (**a**), without significant body weight difference with the nontreated group (**b**). Hematoxylin and eosin (**c**) showing dense cellular networks, except in the PTX-NFM treatment group. TUNEL staining (**d**) of tumor tissues harvested at 14 days after each treatment is indicative for cellular apoptosis. White and yellow scale bars represent 15 and 50 μm, respectively. *P*-values were calculated with student t-tests: * $p<0.05$, ** $p<0.01$

leads to cellular apoptosis. Generally, cells treated with PTX increase populations of G2/M phase cells; however prolonged treatment with PTX over day led to substantial cell death and increased the sub G1 populations of cells (Mo and Lim 2005). Fig. 4 shows, populations of sub G1 cells increased with respect to the non-treated and NFM control groups. The control groups showed cell populations of 4.1 % non-treatment and 5 % NFM in sub G1 while the treated cells showed a 5–6 fold increase at 26.1 % for free PTX-INJ and 29.0 % for PTX-NFM. Figure 5 shows the apoptosis analysis

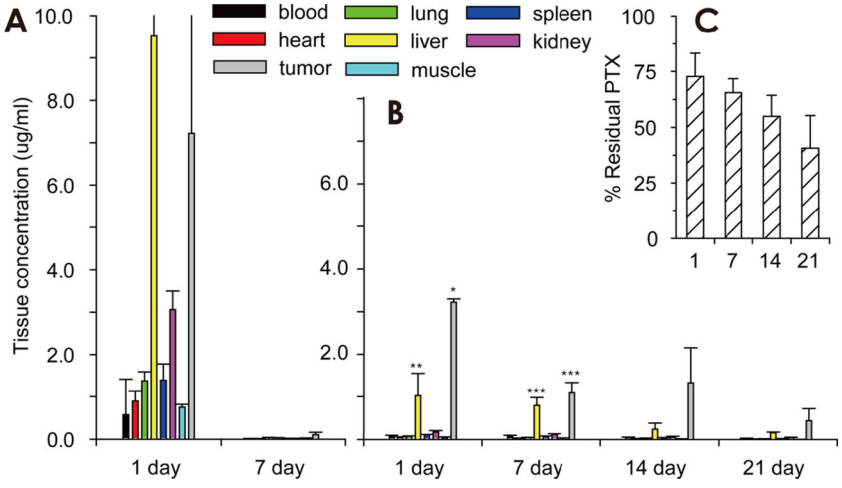

Fig. 7 Tissue distribution of PTX after subtumoral injection of PTX-INJ (**a**) and subtumoral embedding of PTX-NFM (**b**) ($n=4$). (**c**) The residual amount (%) of PTX in the PTX-NFM. P-values are the comparison of PTX concentrations tissue (liver or tumor) between test groups (PTX-INJ and PTX-NFM) on days 1 and 7. *P*-values were calculated using student t-tests: * $p<0.05$, ** $p<0.01$, *** $p<0.001$

of the cells. The non-treated cells showed 3.6 % in early apoptosis and 14.5 % in late apoptosis and necrosis; the PTX-NFM treated group showed 34.7 % of the cell population in early apoptosis and 52.6 % in late apoptosis and necrosis. The PTX-INJ treated cells also showed increased populations in both early and late apoptosis, but those populations were lower than PTX-NFM treatment group. This cellular apoptosis correlated well with the TUNEL analysis of *in vivo* xenografts discussed below (Fig. 6d).

3.3 *In vivo* antitumor efficacy and histological observations

Tumor growth, measured as tumor volume, was inhibited in the PTX-INJ and PTX-NFM treatment groups. We noted that tumor growth for the PTX-NFM group was nearly 1.5-fold greater than the PTX-INJ group at 21 day and nearly 3-fold greater than the NFM control group (Fig. 6a). Overall, the PTX-NFM group maintained normal body mass throughout the experiment (Fig. 6b). No sign of toxicity, such as weight loss, ruffling of fur, or change in behavior and feeding, was detected in PTX-NFM. Two mice in the PTX-INJ group (1.2 mg PTX/mouse; subtumoral injection) died during the experiment that might be from systemic toxicity of PTX.

Tumor tissues were harvested 14 days post injection, stained with H&E dye, and assessed for morphology (Fig. 6c). Tissue samples recovered at the beginning of treatments showed a dense cellular structure. Tumors treated with the PTX-NFM showed distinct alterations in the morphology in H&E staining, while other tissues did not show any significant changes in cellular structures (Fig. 6c). The dense cellular network is less ordered. TUNEL staining was used to show the population of cells undergoing apoptotsis (Fig. 6d). Only a small population of cells was apoptotic in the non-treated and NFM control groups. The PTX-INJ and PTX-NFM resulted in larger populations of apoptotic cells; furthermore, tumors treated with PTX-NFM showed the largest population apoptotic cells than those treated with PTX-INJ.

The PTX-NFM successfully inhibited the proliferation of CT-26 cells both *in vitro* and *in vivo*. The successful delivery of PTX by electrospun nanofibers covered SEMS could be a potential alternative palliative treatment for malignant gastrointestinal cancer as well as cancer-related stenosis.

3.4 Tissue concentration of PTX

The tissue-distribution of PTX was measured in the heart, lung, liver, spleen, kidney, muscle, tumor and blood at 1 and 7 days for PTX-INJ and 1, 7, 14, and 21 days for PTX-NFM (Fig. 7). The sub-tumoral injection of PTX-INJ resulted in higher tissue concentrations of PTX at 1 day post injection. In particular, the liver and tumor showed 9.52±5.84 μg/mL and 7.22±6.94 μg/mL of PTX concentrations, respectively. PTX was only marginally detected in most tissues at 7 days and undetectable at 14 and 21 day post PTX-INJ treatment. Tumoral concentration of PTX at 7 day was 0.10±0.06 μg/mL aftet PTX injection. This concentration was ineffective in preventing tumor growth. However, mice treated with PTX-NFM displayed a sustained tumoral concentration of PTX: 1 day=3.23±0.07 μg/mL, 7 day=1.09±0.24 μg/mL, 14 days=1.33±0.81 μg/mL, and 21 days=0.43±0.28 μg/mL. Concentrations of PTX were generally higher in the tumor that in the liver in the PTX-NFM group. Biodistribution data showed that directional release of PTX was accomplished and the drug was localized in greater concentrations in the tumor as opposed to the liver.

We also measured the remaining PTX in the PTX-NFMs. The imbedded PTX-NFMs were recovered from the tumor, washed with PBS, and dissolved in organic solvents. The solvent was then subjected to HPLC and LC-MS/MS analysis. The data showed that around 35 % of PTX initially burst from PTX-NFM in 1 day. Under *in vivo* conditions, PTX-NFM inevitably contacts the blood circulation, which precipitated the release of PTX. However, after this initial burst, slow systemic release kinetics was observed. The embedded PTX-NFM showed 40.0±14.6 % residual PTX after 21 days. This data correlated with the *in vitro* release studies and suggested that the PTX-NFM can remain for up to 30 day or longer. When it comes to cholangiocarcinoma, we are also investigating whether one month of drug release is enough to extend the patency of the stent. The European Society of Gastrointestinal Endoscopy recommend insertion of SEMS when expected survival time is >4 months or if the cost of the SEMS itself is <50 % than that of ERCP procedure (Dumonceau et al. 2011). The survival time of patients with unresectable malignant biliary obstruction is less than one year (O'brien et al. 1995), so the partial or total regression of tumor for one month or more by PTX eluting EMS poses adequate rationale for further development.

4 Conclusion

We studied paclitaxel-loaded PU nanofiber membrane covered self-expandable metallic stents for the treatment of gastrointestinal cancer and malignant stenosis. The electrospun nanofiber allowed even distribution of PTX on the membrane, favourable release of PTX for 1 month and *in vitro* tumor growth inhibition. The positive results shown here encourage further investigations of PTX-eluting nanofiber-covered SEMS as an alternative biliary intervention for the palliative treatment of cholangiocarcinoma.

Acknowledgments This research was supported by Basic Science Research Program through the National Research Foundation of Korea (NRF) funded by the Ministry of Science, ICT and future Planning

(2014R1A2A2A04006562), and supported by research grant (INHA-47278-01) from INHA UNIVERSITY.

References

M.R. Bennett, In-stent stenosis: pathology and implications for the development of drug eluting stents. Heart **89**, 218–224 (2003)

M.P. Davis, C. Nouneh, Modern management of cancer-related intestinal obstruction. Curr Oncol Rep **2**, 343–350 (2000)

J. Deng, Y. Han, M. Sun, J. Tao, C. Yan, J. Kang, S. Li, Nanoporous CREG-eluting stent attenuates in-stent neointimal formation in porcine coronary arteries. PLoS One **8**, e60735 (2013)

J.M. Dumonceau, D. Heresbach, J. Deviere, G. Costamagna, U. Beilenhoff, A. Riphaus, Biliary stents: models and methods for endoscopic stenting. Endoscopy **43**, 617–626 (2011)

R. Hoffmann, G.S. Mintz, G.R. Dussaillant, J.J. Popma, A.D. Pichard, L.F. Satler, K.M. Kent, J. Griffin, M.B. Leon, Patterns and mechanisms of in-stent restenosis. A serial intravascular ultrasound study. Circulation **94**, 1247–1254 (1996)

G.H. Hsiue, S.D. Lee, P.C. Chang, C.Y. Kao, Surface characterization and biological properties study of silicone rubber membrane grafted with phospholipid as biomaterial via plasma induced graft copolymerization. J. Biomed. Mater. Res. **42**, 134–147 (1998)

S.G. Kang, Gastrointestinal stent update. Gut Liver **4**(Suppl 1), S19–24 (2010)

W. Khan, S. Farah, A.J. Domb, Drug eluting stents: developments and current status. J. Control. Release **161**, 703–712 (2012)

J.H. Kim, Endoscopic stent placement in the palliation of malignant biliary obstruction. Clin Endosc **44**, 76–86 (2011)

T.Y. Kim, D.W. Kim, J.Y. Chung, S.G. Shin, S.C. Kim, D.S. Heo, N.K. Kim, Y.J. Bang, Phase I and pharmacokinetic study of Genexol-PM, a cremophor-free, polymeric micelle-formulated paclitaxel, in patients with advanced malignancies. Clin. Cancer Res. **10**, 3708–3716 (2004)

D.K. Lee, H.S. Kim, K.S. Kim, W.J. Lee, H.K. Kim, Y.H. Won, Y.R. Byun, M.Y. Kim, S.K. Baik, S.O. Kwon, The effect on porcine bile duct of a metallic stent covered with a paclitaxel-incorporated membrane. Gastrointest. Endosc. **61**, 296–301 (2005)

S.S. Lee, J.H. Shin, J.M. Han, C.H. Cho, M.H. Kim, S.K. Lee, J.H. Kim, K.R. Kim, K.M. Shin, Y.H. Won, H.Y. Song, Histologic influence of paclitaxel-eluting covered metallic stents in a canine biliary model. Gastrointest. Endosc. **69**, 1140–1147 (2009)

L. Lei, X. Liu, S. Guo, M. Tang, L. Cheng, L. Tian, 5-fluorouracil-loaded multilayered films for drug controlled releasing stent application: drug release, microstructure, and ex vivo permeation behaviors. J. Control. Release **146**, 45–53 (2010)

D. Manifold, N. Maynard, M. Cowling, L. Machan, R. Mason, A. Adam, Taxol coated stents in oesophageal adenocarcinoma. Gastroenterology **114**, A27 (1998)

J.C. Martinez, M.M. Puc, R.M. Quiros, Esophageal stenting in the setting of malignancy. ISRN Gastroenterol **2011**, 719575 (2011)

Y. Mo, L.Y. Lim, Paclitaxel-loaded PLGA nanoparticles: potentiation of anticancer activity by surface conjugation with wheat germ agglutinin. J. Control. Release **108**, 244–262 (2005)

S. Moon, S.G. Yang, K. Na, An acetylated polysaccharide-PTFE membrane-covered stent for the delivery of gemcitabine for treatment of gastrointestinal cancer and related stenosis. Biomaterials **32**, 3603–3610 (2011)

T. Nicholson, Stents: an overview. Hosp Med **60**, 571–573 (1999)

S. O'brien, A.R. Hatfield, P.I. Craig, S.P. Williams, A three year follow up of self expanding metal stents in the endoscopic palliation of longterm survivors with malignant biliary obstruction. Gut **36**, 618–621 (1995)

J.Y. Park, B.K. Park, J.S. Ko, S. Bang, S.Y. Song, J.B. And Chung, Bile acid analysis in biliary tract cancer. Yonsei Med. J. **47**, 817–825 (2006)

H.B. Park, H. Yoo, T. Hwang, T.J. Park, D.H. Pail, S.W. Choi, J.H. Kim, Fabrication of levofloxacin-loaded nanofibrous scaffolds using coaxial electrospinning. J Pharm Inv **42**, 89–93 (2012)

S. Ramcharitar, P.W. Serruys, Fully biodegradable coronary stents : progress to date. Am J Cardiovasc Drugs **8**, 305–314 (2008)

M.P. Savage, J.S. Douglas Jr., D.L. Fischman, C.J. Pepine, S.B. King 3rd, J.A. Werner, S.R. Bailey, P.A. Overlie, S.H. Fenton, J.A. Brinker, M.B. Leon, S. Goldberg, Stent placement compared with balloon angioplasty for obstructed coronary bypass grafts. Saphenous Vein *De Novo* Trial Investigators. N. Engl. J. Med. **337**, 740–747 (1997)

S. Thurnher, J. Lammer, M. Thurnher, F. Winkelbauer, O. Graf, R. Wildling, Covered self-expanding transhepatic biliary stents: clinical pilot study. Cardiovasc. Intervent. Radiol. **19**, 10–14 (1996)

T. Tsuji, H. Tamai, K. Igaki, E. Kyo, K. Kosuga, T. Hata, T. Nakamura, S. Fujita, S. Takeda, S. Motohara, H. Uehata, Biodegradable stents as a platform to drug loading. Int J Cardiovasc Intervent **5**, 13–16 (2003)